BIOCHEMISTRY
including biophysical chemistry & molecular biology
Article

Biochemistry **2009,** *48,* 7201–7208 7201
DOI: 10.1021/bi900647g

Two Families of Synthetic Peptides That Enhance Fibrin Turbidity and Delay Fibrinolysis by Different Mechanisms[†,‡]

Leela Pandi, Justin M. Kollman,[§] Francisco Lopez-Lira,[∥] Jason M. Burrows, Marcia Riley, and Russell F. Doolittle*

Department of Chemistry and Biochemistry and Division of Biology, University of California at San Diego, La Jolla, California 92093-0314 [§]*Current address: Department Biochemistry and Biophysics, University of California, San Francisco, CA 94518.* [∥]*Current address: Genomic Medicine Laboratory, Ministry of Health of Nayarit, Tepic, Nayarit, Mexico.*

Received April 15, 2009; Revised Manuscript Received June 11, 2009

ABSTRACT: When fibrin clots are formed in vitro in the presence of certain positively charged peptides, the turbidity is enhanced and fibrinolysis is delayed. Here we show that these two phenomena are not always linked and that different families of peptides bring about the delay of lysis in different ways. In the case of intrinsically adhesive peptides corresponding to certain regions of the fibrinogen γC and βC domains, even though these peptides bind to fibrin(ogen) and enhance turbidity, the delay in lysis is mainly due to direct inhibition of plasminogen activation. In contrast, for certain pentapeptides patterned on fibrin B knobs, the delay in lysis is a consequence of how fibrin units assemble. On their own, these B knob surrogates can induce the gelation of fibrinogen molecules. The likely cause of enhanced clot turbidity and delay in fibrinolysis was revealed by a crystal structure of the D-dimer from human fibrinogen cocrystallized with GHRPYam, the packing of which showed the direct involvement of the ligand tyrosines in antiparallel βC−βC interactions.

In blood clots, fibrin is formed when thrombin releases amino-terminal peptides (fibrinopeptides) from fibrinogen, thereby exposing sets of knobs that can interact with holes on neighboring molecules. Synthetic peptides patterned on the A knob of fibrin can prevent polymerization and arrest clot formation (*1*). In contrast, peptides based on B knobs enhance the turbidity of in vitro clots and can delay the onset of tissue plasminogen activator-induced fibrinolysis (*2*, *3*). With regard to the latter, a similar result has been reported for a peptide patterned on the segment of the γC domain of human fibrinogen encompassed by residues γ365−380 (*4*). Here, we inquire about the basis of the delays in fibrinolysis caused by these two different kinds of positively charged peptides. In the end, the delays in lysis were found to be due to completely independent activities. The subject is important because much disagreement about how fibrin stimulates tPA[1] to activate plasminogen remains (reviewed in ref *5*).

In the case of B knob homologues, we had hypothesized that the delay could be due to occupancy of the βC hole by the synthetic B knob, thereby preventing the tethered authentic B knob from holding the βC domain in a conformation providing access for the binding of tPA or plasminogen (*2*). We have now performed additional experiments that suggest such a model is likely not correct. Instead, the data indicate that certain B knob homologues, but not all, lead to specific associations between molecules of fibrin(ogen), causing them to be less vulnerable to destruction.

Independently, longer peptides corresponding to portions of the fibrinogen γC domain were also found to enhance clot turbidity and to delay fibrinolysis (*4*). In that study, 77 overlapping dodecameric peptides were synthesized corresponding to virtually the entire length of the γC domain. Of all those peptides, one (γ369−380) stood out above all the others when measured by thromboelastography. The same peptide also greatly delayed tPA-stimulated fibrinolysis (*4*).

Reports involving synthetic peptides based on this region of the γC domain had appeared earlier, including the finding that essentially the same peptide (γ370−381) is an integrin-binding site for platelets (*6*, *7*), or, in another study, to enhance clotting (*8*). Even earlier, a similar peptide (γ369−376) had been synthesized on the basis of findings of phage display, in which case it was found that sequences involving three tryptophans spaced in the order W-X-X-W-X-X-X-W are remarkably adhesive, or "sticky", and bind tightly to polystyrene (*9*). A computer search for that motif led those authors to the finding that the β and γ chains of vertebrate fibrinogens invariably satisfy this sequence requirement (*9*). Because the β and γ chains of fibrinogen are homologous, we included the β chain equivalent (β437−448) of the γC dodecamer (γ369−376) in our study. The sequences and structural locations of these peptides are shown in Figures S1 and S2 of the Supporting Information.

MATERIALS AND METHODS

The synthetic peptides used in this study were obtained from three different sources; several were from more than one source and

[†]This work was supported in part by Grant HL-81553 from the National Heart, Lung, and Blood Institute and in part by a grant from the American Heart Association. F.L.-L. was supported by a postdoctoral fellowship from UC-MEXUS-CONACYT.

[‡]The atomic coordinates and structure factors for the structure reported in this article have been deposited in the Protein Data Bank as entry 3H32.

*To whom correspondence should be addressed. Telephone: (858) 534-4417. Fax: (858) 534-4985. E-mail: rdoolittle@ucsd.edu.

[1]Abbreviations: GHRPYam, Gly-His-Arg-Pro-Tyr-amide; GHRPam, Gly-His-Arg-Pro-amide; XHRPY, pentapeptide in which X is Gly, Met, Ala or Ser; γW12, dodecapeptide WATWKTRWYSMK from the γ chain of human fibrinogen; γW12am, same peptide as γW12 except with a C-terminal amide; βW12am, β chain dodecapeptide WMNWKGSWYSMR-amide; dVLKpna, D-Val-Leu-Lys-*p*-nitroanilide; PEG, polyethylene glycol; MPD, methylpentanediol; tPA, tissue plasminogen activator; CNBr, cyanogen bromide; CNS, Crystallographic and NMR System; SEM, scanning electron microscopy.

Published on Web 07/01/2009

behaved identically. GPRPam, GHRPam, GHRPLam, and GHRPYam were synthesized by the BOC procedure at the (former) UCSD Peptide Synthesis Facility. Peptide WATWKTRWYSMK was purchased from Sigma-Genosys, as was a mutated version, WATWHDHWYSMK, designed to be refractory to plasmic cleavage. Replacement peptides for ones we had previously synthesized, including GHRPam, GHRPYam, and GHRPLam, were also bought from Sigma-Genosys. The γC and βC homologous peptides WATWKTRWYSMKam and WMNWKGSWYSMRam were purchased from GenScript. The chromogenic peptide dVLKpna was obtained from Sigma Aldrich.

For peptides containing tyrosine or tryptophan, solution concentrations were determined by spectrophotometry; other peptide concentrations were determined either by amino acid analysis or by dry weight. Small portions of some peptides were acetylated by dissolving aliquots in glacial acetic acid and treating them briefly with acetic anhydride at 100 °C, followed by the addition of cold water and freeze-drying. Removal of the carboxyl-terminal lysine from the γW12am peptide was accomplished by treatment with CNBr in 70% formic acid; the completeness of the reaction was ascertained by paper electrophoresis.

Proteins. Fibrinogen was purified from outdated blood bank plasma by a cold ethanol method (*10*). Although the preparations were more than 95% clottable, they contained observable amounts of fibronectin and biologically active amounts of plasminogen and factor XIII. Accordingly, some experiments were conducted on material that had been purified further by DEAE chromatography (*11*, *12*). Additionally, some experiments were conducted with plasminogen-free fibrinogen purchased from CalBiochem.

The fibrin fragment D-dimer (also known as double-D) was prepared from Factor XIII-cross-linked fibrin by limited tryptic digestion (*13*). Plasminogen was prepared from outdated blood bank plasma by affinity chromatography on lysine-Sepharose (*14*). Plasmin was obtained from Chromagenix and thrombin from Enzyme Research; the tPA used was obtained from Sigma-Aldrich and was also a kind gift from T. Morris of the Department of Medicine, University of California at San Diego. Streptokinase was obtained from Sigma.

Turbidity Assays. Turbidity assays were performed in disposable cuvettes in a Helios UV−visible spectrophotometer at 350 nm. Assays involving a tPA/plasminogen mixture-induced fibrinolysis were performed as described previously (*2*). Briefly, unchromatographed fibrinogen (final concentration of 1.0 mg/mL, 0.135 M NaCl, 0.04 M imidazole buffer, pH 7.0) containing plasminogen was mixed with an appropriate peptide and a solution of thrombin and tPA (final concentrations of 0.08 and 0.29 μg/mL, respectively) added at time zero. Alternatively, in some experiments, plasminogen-free fibrinogen was used and purified plasminogen added. In all cases, the final volume was 900 μL. Delays in lysis were calculated on the basis of half-lysis times as described previously (*3*).

In the cases of peptide-induced association assays, peptides were mixed with fibrinogen at time zero and the association was monitored at 350 nm. In some experiments, assays were conducted at multiple wavelengths to determine the nature of the scattering material (*15*−*17*).

Microtiter plate assays were conducted in triplicate. Readings were taken with a TECAN M200 automatic plate reader. In the case of preformed clots, clots were formed by the addition of thrombin to fibrinogen containing various peptides (final volume of 100 μL) and left to stand for 18 h, after which 100 μL of an active enzyme solution was overlaid and the progress of lysis followed in the plate reader. The various proteases tested included trypsin, plasmin, and a tPA/plasminogen mixture.

Scanning Electron Microscopy. Scanning electron microscopy (SEM) was used to investigate the fibrous nature of peptide-induced gels and was conducted at the UCSD Engineering Nano3 Facility. Samples were prepared in a manner similar to that described by Weisel and Nagaswami (*18*). Aliquots of fibrinogen solutions were pipetted into 25 μL Plexiglas microdialysis cells immediately after peptide addition or, for the sake of comparison, after thrombin addition, allowing gels or clots to form in situ. After a suitable time under humidified conditions, samples were washed with saline and fixed with glutaraldehyde, and then passed through a progressive series of ethanol solutions, from 20 to 95%, after which they were stored in absolute ethanol until being subjected to critical point drying. Samples were sputtered with chromium and then examined in a Phillips XL30 ESEM scanning electron microscope.

Crystallography. Crystals were grown at room temperature from sitting drops containing equal volumes of 5 mg/mL D-dimer in 0.05 M Tris (pH 7.0) and 5 mM $CaCl_2$, containing 0.5 mM GHRPYam and 0.3 mM GPRPam, and a well solution composed of 0.05 M Tris (pH 8.0) containing 1% PEG-3350, 1.0 mM iodoacetamide, 1.0 mM $CaCl_2$, and 2 mM sodium azide. Typically, small plates appeared in 1 or 2 days and continued to grow over the course of 1−2 weeks, after which they were harvested. MPD was added gradually as a cryoprotectant to a final concentration of 15%, and crystals were cooled with liquid nitrogen and stored in a Dewar with liquid nitrogen.

Preliminary X-ray diffraction data were collected at the UCSD X-ray Crystallography Facility. Higher-resolution data were collected at the Advanced Light Source, Lawrence Berkeley National Laboratory (Berkeley, CA), beamline 5.0.3. Data were processed with HKL2000 or Denzo and Scalepack (*19*). The structure was determined by molecular replacement using AMoRe (*20*) as described in the CCP4 package (*21*). Model reconstructions were made with the O modeling program package (*22*), and refinement was conducted with CNS (*23*). Ellipsoidal truncation was conducted with the UCLA web server (www.doe-mbi.ucla.edu/~sawaya/anisoscale/anisotropy) (*24*). Structure quality was checked periodically with PROCHECK (*25*). Illustrations were prepared with the aid of PyMol (*26*).

RESULTS

High Concentrations of GHRPam Do Not Delay Fibrinolysis. In an earlier report on synthetic B knobs delaying fibrinolysis (*2*), we compared GHRPam, GHRPLam, and GHRPYam, all at 100 μM. Although all three peptides enhanced turbidity, the delays in lysis were much stronger for the pentapeptides. No effort was made to test the tetrapeptide (GHRPam) at higher concentrations to show that it also delayed fibrinolysis, as opposed to merely enhancing turbidity. We have now performed the experiment and found that, even at 4 mM, GHRPam does not delay lysis significantly (Table 1 and Figure S3 of the Supporting Information), even though it renders clots distinctly more turbid, indicating that occupancy of the βC hole by a surrogate B knob that prevents binding of the authentic B knob is not the cause of the delayed lysis reported previously (*2*). Instead, as developed more fully below, the binding of tyrosyl-ending pentapeptides leads to intermolecular associations between

Table 1: Delays in Fibrinolysis Caused by Various Agents

mixture[a]	Half-Lysis Ratio[b]
control (no additive)	1.00
4000 mM GHRPam	1.14
100 μM GHRPYam	1.65
20 μM γW12	2.52
20 μM γW12 and 100 μM GHRPYam	4.63
100 μM tranexamic acid (TX)	2.86
100 μM TX and 100 μM GHRPYam	6.54
100 μM TX and 20 μM γW12	4.37
100 μM GHRPYam[c]	1.6
20 μM γW12[c]	3.3

[a] Unchromatographed fibrinogen treated with t-PA and thrombin; detailed solution conditions described in the text. [b] Ratios are half-lysis times of experiment to control. [c] t-PA replaced by streptokinase.

fibrin(ogen) units that are likely the cause of the observed delay in lysis.

GHRPYam and γW12 Both Delay Fibrinolysis. In an assay in which fibrin formation and lysis are observed consecutively, and in which all the components are present at time zero, the dodecapeptide γW12 is a much better inhibitor of lysis than GHRPYam is (Figure 1 and Table 1). Moreover, when the two peptides are both present, the effect is more than additive (Table 1). The same general results are obtained when streptokinase is substituted for t-PA (Figures S4 and S5 of the Supporting Information).

The presence of 100 μM tranexamic acid (TX), an inhibitor of fibrinolysis that acts by binding to plasminogen (*27*, *28*), greatly extends the delay in fibrinolysis caused by GHRPYam (Figure 2 and Table 1). In contrast, when TX and γW12 are both present, the effect is less than additive (Table 1), suggesting that tranexamic acid and the γW12 peptide may be competing for plasminogen. The observation led directly to the finding that the γW12 peptide at concentrations as low as 25 μM suppresses fibrin-independent tPA activation of plasminogen in a chromogenic assay, whereas 200 μM GHRPYam has no effect at all (Figure 3A). The γW12 peptide also inhibits plasmin, but not nearly to the same degree (Figure 3B).

Other W12 Peptides. Several peptides related to γW12 were studied in an effort to find how these materials act, with regard to their ability to enhance clot turbidity, on one hand, or to delay lysis, on the other. These included acetylated γW12 (AcγW12), a carboxy-terminal amidated version of γW12 (γW12am), a CNBR-treated version of γW12am in which cleavage at the penultimate methionine residue removed the carboxy-terminal lysine (CbγW12am), a mutated version of γW12 with three amino acid substitutions (MuγW12), βW12am, and a CNBr version of βW12am (CbβW12am) (Table 2).

Acetylation of the three amino groups in γW12 greatly reduced the peptide's effectiveness, both in enhancing turbidity and in delaying lysis (Table 2), but not to the point where it was less active than GHRPYam on a molar basis in slowing lysis (Figure S6 of the Supporting Information). In contrast, amidation of the carboxy terminus of γW12 greatly increased the effectiveness of the peptide in all respects (Table 2 and Figure S7 of the Supporting Information). CNBr treatment of this latter peptide reduced its effectiveness in both kinds of test, but only to the point where its activity was approximately the same as that of γW12 (Table 2 and Figure S8 of the Supporting Information). The βW12am peptide was actually more active than γW12 with

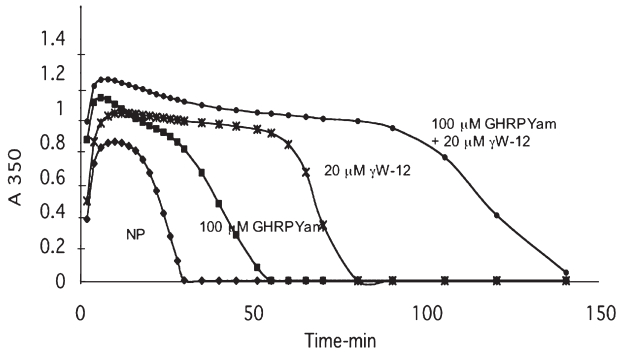

FIGURE 1: Comparison of GHRPYam (100 μM) and γW12 (20 μM) in delaying tPA-stimulated fibrinolysis. Thrombin and tPA were added at zero time. NP means no peptide. When 100 μM GHRPYam and 20 μM of γW12 are both present, the effect is more than additive (see also Table 1).

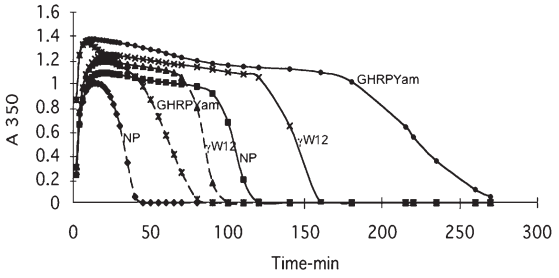

FIGURE 2: Influence of tranexamic acid (100 μM) on the effectiveness of GHRPYam (100 μM) and γW12 (20 μM) in delaying tPA-stimulated fibrinolysis (see Materials and Methods). The dashed lines denote the absence of tranexamic acid; the solid lines denote the presence of tranexamic acid. NP means no peptide (see also Table 1).

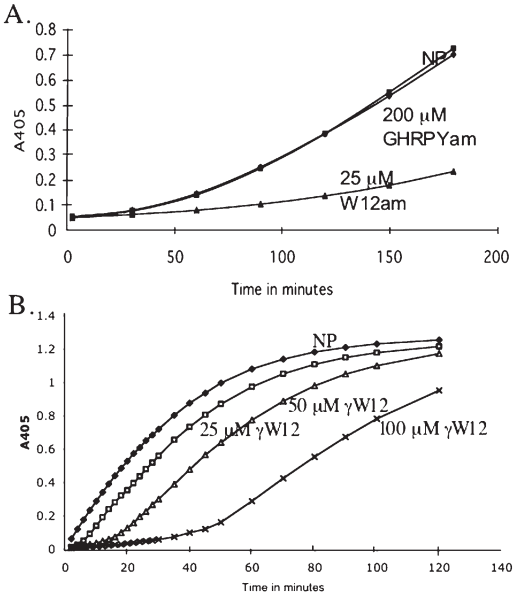

FIGURE 3: (A) Fibrin-independent generation of plasmin in the presence of GHRPYam (200 μM) or γW12 (25 μM) as measured by a chromogenic assay conducted under the same conditions of clotting-lysis assays except fibrinogen was omitted. (B) Effect of γW12 on plasmin acting on a chromogenic substrate.

regard to increasing clot turbidity, but it was only modestly effective in delaying fibrinolysis (Table 2 and Figure S9 of the Supporting Information), an observation consistent with clot

Table 2: Relative Effectiveness of Various "W12 Peptides"[a]

designation (sequence)	net charge	enhanced turbidity	delayed lysis	enhanced PI[b] gelation
γW12 (WATWKTRWYSMK)[c]	+3	1.00	1.00	1.00
γW12am (WATWKTRWYSMKam)[d]	+4	1.92	1.27	1.97
AcγW12 [$(Ac)_3$WATWKTRWYSMK][e]	0	0.62	0.68	0.62
CbγW12am (WATWKTRWYSHse)[f]	+2	1.33	0.74	0.40
MuW12 (WATWHDHWYSMK)[g]	δ+	0.99	0.76	0.53
βW12am (WMNWKGSWYSMRam)[h]	+3	2.02	0.42	1.32
CbβW12am (NWKGSWYSHse)[i]	+1	0.47	0.21	not done

[a] All values scaled to those of γW12 set at 1.00. [b] PI indicates peptide-induced polymerization of fibrinogen by GHRPYam or other XHRPYam peptides. [c] γW12 represents human fibrinogen γ chain residues 369−380. [d] Same as γW12 except amidinated carboxy terminus. [e] Same as γW12 except all three amino groups acetylated. [f] Same as γW12am except carboxy-terminal lysine removed by CNBr; Hse is homoserine. [g] Same as γW12 except residues 5−7 (KTR) replaced by HDH. [h] Homologous region of the human fibrinogen β chain; amidinated carboxy terminus. [i] CNBr-treated βW12 leading to a 9-mer with homoserine.

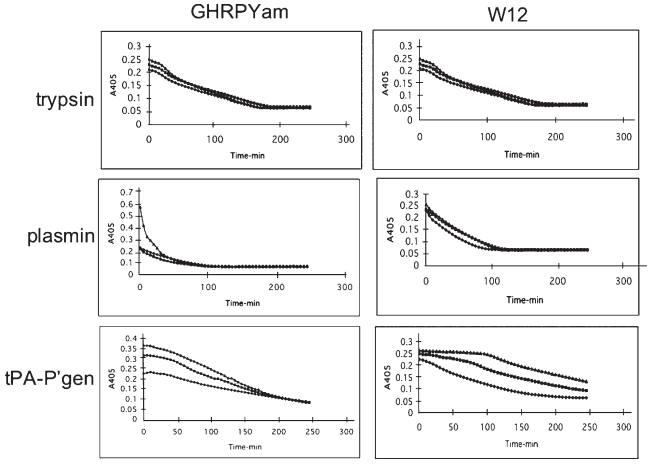

FIGURE 4: Comparison of the effectiveness of GHRPYam (left) and γW12 (right) in delaying lysis of preformed clots on microtiter plates (clots formed in presence of peptide as well as being included at the same concentration in the protease overlay) by trypsin, plasmin, or the tPA−plasminogen combination. In the GHRPYam clots, the concentrations of peptide were 0 (◆), 100 (▲), and 200 μM (■). In the γW12 clots, the peptide concentrations were 0 (◆), 50 (▲), and 100 μM (■). The only significant delay was the γW12 inhibition of lysis by the tPA−plasminogen combination (bottom right).

turbidity and lysis delay effects caused by W12 peptides being independent of each other.

Lysis of Preformed Clots. Preformed clots on microtiter plates were overlaid with trypsin, plasmin, or the tPA−plasminogen combination, and the influence of various peptides was examined with regard to the course of fibrinolysis. Lysis was delayed by the γW12 peptide, but GHRPYam was not effective (Figure 4). The results were the same whether the various peptides were present in the fibrinogen when the clots were formed. The γW12 peptide did not inhibit the destruction of the fibrin clots by trypsin and only to a small degree with plasmin (Figure 4), consistent with the notion that these peptides, like tranexamic acid, bind to subsidiary domains of plasminogen and not to the catalytic site.

Crystal Structure and Packing. Crystals of D-dimer cocrystallized with GHRPYam were limited to small thin plates, and it was only possible to collect data to 3.6 Å resolution (Table 3). Electron density maps were clear, however, and the GHRPYam ligands were obvious in both βC holes, but not in the γC holes. The small amounts of GPRPam (0.3 mM) needed during crystallization were sufficiently low that this ligand appeared in only one of the γC holes in $F_o - F_c$ maps (F chain).

Table 3: Data Collection and Refinement Statistics for DD-GHRPY

space group	*C*2
unit cell	
a (Å)	264.74
b (Å)	97.32
c (Å)	132.50
β (deg)	122.8
highest resolution (Å)	3.6 (3.53−3.66)[a]
no. of observations	110824
no. of unique reflections	31584 (2075)[a]
completeness (%)	89.4 (59.0)[a]
redundancy	3.6 (2.9)[a]
$R_{sym}(I)$[b]	0.073 (0.310)[a]
mosaicity (deg)	0.4
no. of reflections submitted for anisotropy	30310
no. of reflections removed by ellipsoidal truncation	5308
no. of reflections after truncation	25002
isotropic *B* factor (Å^2)	−48.1
refinement resolution range (Å)	50−3.6
no. of amino acid residues in protein	1478
no. of amino acid residues in model	1356
R factor[c]	0.2631
R_{free}[d]	0.3199
root-mean-square deviation for ideal bond lengths (Å)	0.0130
root-mean-square deviation for bond angles (deg)	1.679

[a] Values in parentheses describe data for the highest-resolution shell. [b] $R_{sym} = (\sum|I - \langle I\rangle|)/(\sum|I|)$. [c] Crystallographic *R* factor $[(\sum||F_o| - |F_c||)/\sum|F_o|]$ with 95% of the native data. [d] R_{free} is the *R* factor based on 5% of the native data withheld from the refinement.

The carbohydrate clusters at βAsn364 were prominent, eight of 11 sugars being positioned in both locations.

The molecular packing is completely different from what has been reported for D-dimer cocrystallized with GHRPam or GPRPam. Similarly, DD-GHRPam crystals soaked with GHRPYam naturally retained the original GHRPam lattice, a form in which the D-dimers are bent across the D−D interface compared with other D-dimer structures (*29*). In contrast, the DD-GHRPYam cocrystal has the more extended form observed for D-dimer crystallized without peptide ligands (*29*). The most significant difference, however, is that in the cocrystal the βC domains are packed against each other in a reciprocal and antiparallel fashion (Figure 5). Electron density maps clearly show an interaction between the terminal tyrosines of the peptide ligand and neighboring molecules in the crystal (Figure 6).

Peptide-Induced Gelation of Fibrinogen. When GHRPYam is added to a fibrinogen solution, a mild turbidity becomes evident over the course of 20−30 min, the strength and speed of the response depending on the concentration of the peptide,

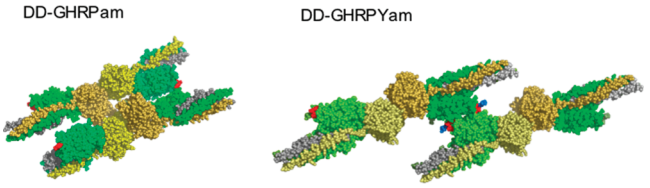

FIGURE 5: D-Dimer cocrystallized with GHRPam (Protein Data Bank entry 1FZF) packs differently than does D-dimer cocrystallized with GHRPYam. In particular, the latter has an antiparallel, symmetrical, $\beta-\beta$ interface. Red spheres correspond to the GHRPYam ligand; blue regions denote the first two sugars of the carbohydrate cluster: α chains, gray; β chain, green; γ chain, gold.

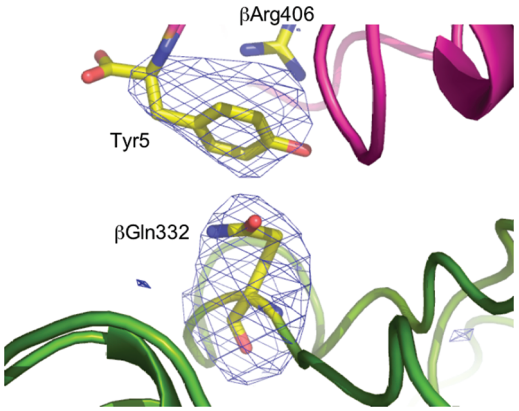

FIGURE 6: $F_o - F_c$ electron density map of D-dimer cocrystallized with GHRPYam showing how the tyrosine ring of the peptide extends to the side chain of βGln332 on the neighboring molecule. A reciprocal interaction occurs at the other end of the interface (see Figure 5). The map is contoured at 2.7σ; the Tyr and Gln residues were not included in the calculation. The interaction between Tyr5 of the ligand and the βC hole has been shown to be stabilized by interaction of the ring and the guanidine group of βArg406 (*3*). The magenta backbone is from the host β chain; the green backbone is from the β chain of the neighboring molecule.

the concentration of fibrinogen, and the pH (Figure 7). Turbidity does not result upon the addition of γW12. When it is added together with GHRPYam, however, a greatly enhanced turbidity is generated (Figure 7); the enhancement is even greater with γW12am (Figure S10 of the Supporting Information).

Even more remarkable is the fact that all of the solutions containing GHRPYam, whether or not W12 peptides were present, gelled to the point where tubes could be inverted without flow. Moreover, other members of the XHRPYam family are also effective (Figure S11 of the Supporting Information), more or less in proportion to their effectiveness in delaying lysis, although only a few of the peptides characterized in a previous study (*3*) were tested. The tetrapeptide GPRPam, an antipolymerant, diminished the turbidity of XHRPYam-induced systems, presumably by competing with the XHRPYam peptides for the βC hole.

The wavelength dependence of the turbidity induced by these peptides was consistent with the generation of fibers rather than a flocculent precipitate (Figure S12 of the Supporting Information), an observation confirmed by scanning electron microscopy (Figure 8).

DISCUSSION

Over the years, there have been countless studies of the influence of environmental factors on the character of

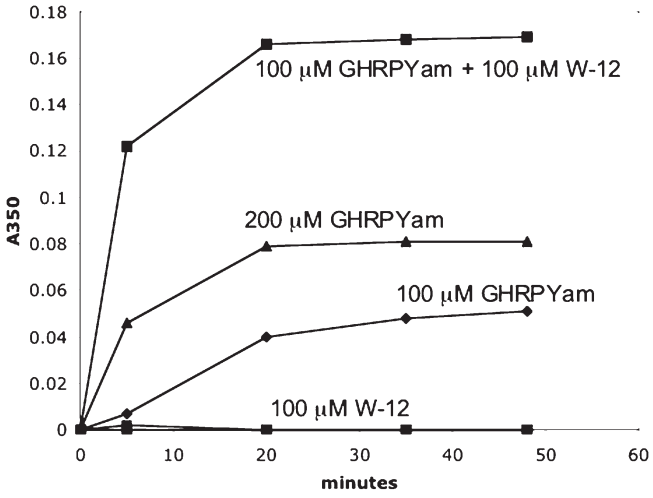

FIGURE 7: Turbidity of a fibrinogen solution [1 mg/mL in 0.15 M NaCl and 0.05 M imidazole buffer (pH 7.0)] induced by GHRPYam at concentrations of 100 and 200 μM. The γW12 peptide does not induce turbidity on its own (concentration of 100 μM), but it enhances that induced by GHRPYam. All solutions containing GHRPYam gelled to the point where cuvettes could be inverted without observable flow.

thrombin-catalyzed fibrin clots. In brief, coarse (turbid) clots, which have more extensive lateral associations than fine clots (*30*), are favored under conditions of low ionic strength or low pH and many other circumstances, including the presence of calcium ions, removal of fibrinopeptides B, and the removal of sialic acids. Kinetic factors also play a role in how fibrin assembles, and the less thrombin supplied under a given set of conditions, the slower the polymerization and the more turbid the final product (*31*, *32*).

In general, coarse clots are lysed more rapidly than fine clots (*31*–*34*). However, clots formed in the presence of certain synthetic peptides based on B knobs (*2*, *3*) and another set based on a section of the γC domain ("W12 peptides") (*4*) appear to be exceptions to this rule. Both kinds of peptides enhance the turbidity of fibrin and delay tPA-provoked fibrinolysis, but they do so by completely different mechanisms.

W12 Peptides. The basis for how the γ chain W12 peptides delay lysis is now clear; these peptides inhibit the conversion of plasminogen to plasmin. It is doubtful that their effectiveness depends on the presence of lysine, a common feature of many plasmin(ogen) inhibitors, because even fully acetylated peptides retain some activity, and a mutant peptide without lysine was also effective (Table 2). The fact that γW12am is significantly more effective than γW12 shows that the unamidated carboxy-terminal lysine is definitely not involved. Complete removal of the carboxy-terminal lysine by cyanogen bromide diminishes the effectiveness of this peptide for enhancing turbidity, but only to the extent that it matches the similarly charged γW12 (Table 2).

In the end, γ chain W12 peptides were shown to exhibit two independent activities: they interfere with the generation of plasmin, but they also bind to fibrin(ogen) and enhance both the turbidity of fibrin clots and the XHRPY-induced association of fibrinogen. In the latter roles, they do not generate fibers on their own. The more net positive charge any of these peptides carry, the greater their enhancing effect on clot turbidity and the XHRPYam inducement of fibrinogen polymerization (Table 2).

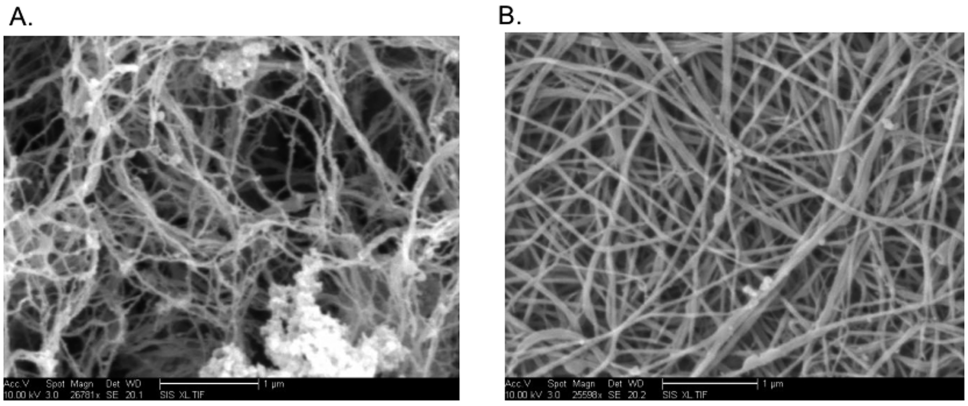

FIGURE 8: (A) Scanning electron micrograph of a gel produced by incubating GHRPYam with human fibrinogen. Solution conditions as described in the legend of Figure 7. (B) Control preparation of fibrinogen clotted with thrombin. In both cases, the magnification is approximately 27000×. The scale bar is 1 μm.

There was no direct correspondence between a peptide's ability to enhance turbidity and the extent of delay in fibrinolysis. As an example, βW12am greatly enhances the turbidity of thrombin-generated fibrin clots, but it is not nearly as effective as γW12 or γW12am in delaying tPA-activated fibrinolysis by plasminogen (Table 2 and Figure S9 of the Supporting Information).

The question of whether the enhanced clot turbidity and suppression of plasmin generation induced by these peptides are merely consequences of the unusual adhesiveness associated with this constellation of amino acids arises (*9*). Whether or not this is the case, it is remarkable that, on a molar basis, these peptides inhibit plasmin generation more effectively than tranexamic acid, a highly touted inhibitor (*27*, *28*).

Synthetic B Knobs. The mechanistic basis for slower fibrinolysis with the tyrosine-containing B knobs is completely different from the case of the γ chain W12 peptides and instead has to do with the way fibrin is assembled. The likely cause of this alternative assembly was revealed by an X-ray structure of D-dimer cocrystallized with GHRPYam that showed a novel set of intermolecular contacts compared with what had been previously observed when GHRPYam was soaked into preexisting D-dimer crystals (*3*). What was lacking in that previously determined crystal structure was any information about how the binding of the peptide might affect interactions in solution with other molecules. The structure of D-dimer cocrystallized with GHRPYam confirms an interaction with βArg406 and shows further that the tyrosine also interacts with neighboring molecules, leading to a crystal with novel packing with βC−βC interfaces. The interaction involves β chain residues 332−362, which are homologous to γ chain residues 268−298, a key segment at the D−D interface. In the case of the βC−βC situation, however, the abutting molecules are oriented in a symmetrical, antiparallel fashion. Almost certainly, the GHRPYam-induced association of fibrinogen molecules, which leads to a fibrous network (Figure 8), must be the result of this same set of βC interactions. Not surprisingly, the most active of the XHRPYam peptides with regard to delaying fibrinolysis by the tPA−plasminogen system (*3*) are also the best at inducing fibrinogen association.

Antiparallel interfaces between βC domains at this stage would prevent the kind of lateral associations proposed in a model of fibrin formation (*35*); it may be that this alternative arrangement slows the normal course of fibrinolysis, either by inhibiting access to critical targets or by occluding important binding sites for tPA, SK, or plasminogen. The fact that half-lysis times are approximately doubled when these peptides are at saturating concentrations might suggest that half of such critical sites have been rendered inaccessible.

If the basis of the XHRPYam-caused delay in lysis is in fact alternatively assembled fibrin, several previously enigmatic observations can be explained, including the exaggerated turbidity and lysis delay observed with batroxobin-induced clots, as well as delayed lysis of fibrin clots when plasmin is substituted for the tPA−plasminogen system (*2*). It also explains the exaggerated additivity of lysis delay observed when either tranexamic acid or γ chain W12 peptides are present. The extent of plasmin generation is reduced, and the plasmin that does emerge encounters a less vulnerable form of fibrin. All of these results are consistent with delay caused by misassembly.

A new, but small, anomaly may be the lack of inhibition observed when plasmin or tPA−plasminogen mixtures are overlaid on preformed clots made in the presence of GHRPYam (Figure 4). This may be attributable to the difference between experiments in which all the components are present at the start (endogenous) and the overlay experiments in which the proteases are provided from without (exogenous) and where the rate of lysis is diffusion-limited. Others have commented on these distinctions in the past (*34*).

As an aside, it should be noted that bovine fibrinogen appears to be unique in having a tyrosine at position 5 of its B knob; 16 of 17 sequences available from different vertebrates have either Leu or Val at that position. The peptide GHRPLam is not nearly as effective as GHRPYam in enhancing clot turbidity and delaying tPA activation of plasminogen (*2*), requiring a 10-fold higher concentration of GHRPLam to give the same delay in lysis that is achieved by GHRPYam. It seems unlikely that the presence of tyrosine at this position in bovine fibrinogen, where it is a part of the long tether extending to the B knob, leads to significant differences from other fibrins; further experiments may be illuminating.

It is possible that the addition of the tyrosine residue to the synthetic B knobs merely provides additional stabilization for a kind of association that does in fact occur during natural fibrin formation. In fact, the very same crystal packing observed for D-dimer cocrystallized with GHRPYam was recently found in a crystal structure of human fibrinogen with bound GPRPam and GHRPam (*36*).

All these observations support the notion that XHRPYam peptides, which have a +2 charge, induce fibrinogen molecules to

associate in a continuous network on their own by way of the antiparallel association of βC domains from different molecules. The network is further promoted by the binding of the generally adhesive (and positively charged) W12 peptides, which in turn enhances the turbidity by additional lateral association.

In summary, the enhanced turbidity and delayed fibrinolysis observed in fibrin clots formed in the presence of GHRPYam are apparently the result of the way in which protofibrils associate. The association involves antiparallel interactions between the βC domains of neighboring molecules and can be induced even in the absence of thrombin. In contrast, the turbidity of clots formed in the presence of W12 peptides depends on apparently nonspecific binding of these peptides to fibrin(ogen), but the delay in lysis is due to these peptides inhibiting the conversion of plasminogen to plasmin.

ACKNOWLEDGMENT

We thank R. G. Fahey for the use of his microtiter plate reader and T. Morris and J. J. Marsh for a gift of tPA. We are also grateful to Jack Kyte for reading the manuscript and making helpful comments.

SUPPORTING INFORMATION AVAILABLE

Sequences in the γC and βC domains of fibrinogen contain three identically spaced tryptophans (Figure S1). Model of fragment D of human fibrinogen (from Protein Data Bank entry 1FZC) showing locations of homologous γ and β dodecapeptides (Figure S2). The tetrapeptide GHRPam does not delay fibrinolysis at concentrations as high as 4.0 mM under conditions where 0.1 mM GHRPYam doubles the half-lysis time (Figure S3). Streptokinase can substitute for tPA in the activation of plasminogen, and lysis is still delayed by GHRPYam (Figure S4). γW12 peptides delay fibrinolysis in streptokinase-activated plasminogen systems, just as they do in tPA-activated ones (Figure S5). Acetylation of γW12 inhibits its ability to enhance clot turbidity and delay lysis (Figure S6). Carboxy-terminal amidation of the dodecapeptide γW12 enhances clot turbidity and increases delays in fibrinolysis (Figure S7). Cyanogen bromide treatment of γW12am removes the carboxyl-terminal lysine and weakens its ability to delay fibrinolysis (Figure S8). βW12am delays the onset of fibrinolysis of thrombin-generated fibrin in the tPA−plasminogen system (Figure S9). The γW12am peptide enhances the GHRPYam-induced association of fibrinogen more than γW12 does (Figure S10). The MHRPYam peptide induces the association of fibrinogen, and the response is enhanced by γW12 (Figure S11). The wavelength dependence of turbidity is characteristic of fibers with low mass-to-length ratios in that plots of turbidity (2.3 × "absorbance") versus the cube root of the wavelength pass through the origin (*17*) (Figure S12). This material is available free of charge via the Internet at http://pubs.acs.org.

REFERENCES

1. Laudano, A. P., and Doolittle, R. F. (1978) Synthetic peptide derivatives that bind to fibrinogen and prevent the polymerization of fibrin monomers. *Proc. Natl. Acad. Sci. U.S.A. 75*, 3085–3089.
2. Doolittle, R. F., and Pandi, L. (2006) Binding of synthetic B knobs to fibrinogen changes the character of fibrin and inhibits its ability to activate tissue plasminogen activator and its destruction by plasmin. *Biochemistry 45*, 2657–2667.
3. Doolittle, R. F., and Pandi, L. (2007) Probing the β-chain holes of fibrinogen with synthetic peptides that differ at their amino termini. *Biochemistry 46*, 10033–10038.
4. Demple, C.-E., Bindeballe, N., Munchback, M., Blume, C., Borggrefe, M., and Mosesson, M. W. (2007) Changes in fibrinogen and fibrin induced by a peptide analog of fibrinogen γ365−380. *J. Thromb. Haemostasis 5*, 1707–1714.
5. Doolittle, R. F. (2008) Searching for Differences Between Fibrinogen and Fibrin That Affect the Initiation of Fibrinolysis. *Cardiovasc. Hematol. Agents Med. Chem. 6*, 181–189.
6. Podolnikova, N. P., Yakybenko, V. P., Volkov, G. L., Plow, E. F., and Ugarova, T. P. (2003) Identification of a novel binding site for plaetlet integrins $\alpha_{IIb}\beta_3$ (GPIIbIIIa) and $\alpha_5\beta_1$ in the γC-domain of fibrinogen. *J. Biol. Chem. 278*, 32251–32528.
7. Podolnikova, N. P., Gorkun, O. V., Loreth, R. M., Yee, V. C., Lord, S. T., and Ugarova, T. P. (2005) A cluster of basic amino acid residues in the γ370−381 sequence of fibrinogen comprises a binding site for platelet integrin $\alpha_{IIb}\beta_3$ (glycoprotein IIb/IIIa). *Biochemistry 44*, 16290–16930.
8. Marx, G., Ben-Moshe, M., Magdassi, S., and Gorodetsky, R. (2004) Fibrinogen C-terminal peptide sequences (Haptides) modulate fibrin polymerization. *Thromb. Haemostasis 91*, 43–51.
9. Gebhardt, K., Lauvrak, V., Babaie, E., Eijsink, V., and Lindquist, B. H. (1996) *Pept. Res. 9*, 269–278.
10. Doolittle, R. F., Schubert, D., and Schwartz, S. A. (1967) Amino acid sequence studies on artiodactyls fibrinopeptides. I. Dromedary camel, mule deer and Cape Buffalo. *Arch. Biochem. Biophys. 118*, 456–467.
11. Finlayson, J. S., and Mosesson, M. W. (1963) Heterogeneity of human fibrinogen. *Biochemistry 2*, 42–46.
12. Mosesson, M. W., Finlayson, J. S., Umfleet, R. A., and Galanakis, D. (1972) Human fibrinogen heterogeneities. I. Structural and related studies of plasma fibrinogens which are high solubility catabolic intermediates. *J. Biol. Chem. 247*, 5210–5219.
13. Spraggon, G., Everse, S. J., and Doolittle, R. F. (1997) Crystal structures of fragment D from human fibrinogen and its crosslinked counterpart from fibrin. *Nature 389*, 455–462.
14. Deutsch, D. G., and Mertz, E. T. (1970) Plasminogen: Purification from human plasma by affinity chromatography. *Science 170*, 1095–1096.
15. Carr, M. E., and Herman, J. (1978) Size and density of fibrin fibers from turbidity. *Macromolecules 11*, 46–50.
16. Camerini-Otero, R. D., and Day, L. A. (1978) The wavelength dependence of turbidity of solutions of macromolecules. *Biopolymers 17*, 2241–2249.
17. Carr, M. E., and Gabriel, D. A. (1980) Dextran-induced changes in fibrin fiber size and density based on wavelength dependence of gel turbidity. *Macromolecules 13*, 1473–1477.
18. Weisel, J. W., and Nagaswami, C. (1992) Computer modeling of fibrin polymerization kinetics correlated with electron microscope and turbidity observations: Clot structure and assembly are kinetically controlled. *Biophys. J. 63*, 111–128.
19. Otwinowski, Z., and Minor, W. (1997) Processing of X-ray diffraction data collected in oscillation mode. *Methods Enzymol. 276*, 307–326.
20. Navaza, J. (2001) Implementation of molecular replacement in AmoRe. *Acta Crystallogr. D57*, 1367–1372.
21. Collaborative Computational Project Number 4 (1994) . *Acta Crystallogr. D50*, 760–763.
22. Jones, T. A., Zou, J. Y., Cowan, S. W., and Kjeldgaard, M. (1991) Improved methods for building proteins in electron density maps and the location of errors in these models. *Acta Crystallogr. A47*, 110–119.
23. Brunger, A. T., Adams, P. D., Chlore, G. M., DeLano, W. L., Gros, P., Grosse-Kunstleve, R. W., Jiang, J.-S., Kuszewski, J., Nilges, M., Pannu, N. S., Read, R. J., Rice, L. M., Simonson, T., and Warren, G. L. (1998) Crystallography and NMR system: A new software suite for macromolecular structure determination. *Acta Crystallogr. D54*, 905–921.
24. Strong, M., Sawaya, M. R., Wang, S., Phillips, M., Cascio, D., and Eisenberg, D. (2006) Toward a structural genomics of complexes: Crystal structure of a PE/PPE protein complex from *Mycobacterium tuberculosis*. *Proc. Natl. Acad. Sci. U.S.A. 103*, 8060–8065.
25. Laskowski, R. A., MacArthur, M. W., Moss, D. S., and Thornton, J. M. (1993) PROCHECK: A program to check the stereochemical quality of protein structures. *J. Appl. Crystallogr. 26*, 283–291.
26. Delano, W. L. (2002) The PyMOL Molecular Graphics System, DeLano Scientific, San Carlos, CA.
27. Iwamoto, M. (1975) Plasminogen-plasmin system IX. Specific binding of tranexamic acid to plasmin. *Thromb. Diath. Haemorrh. 33*, 573–585.
28. Markus, G., Priore, R. L., and Wissler, F. C. (1979) The binding of tranexamic acid to native (Glu) and modified (Lys) human plasminogen and its effect on conformation. *J. Biol. Chem. 254*, 1211–1216.

29. Everse, S. J., Spraggon, G., Veerapandian, L., and Doolittle, R. F. (1999) Conformational changes in fragments D and double-D from human fibrin(ogen) upon binding the peptide ligand Gly-His-Arg-Pro-amide. *Biochemistry 38*, 2941–2946.
30. Ferry, J. D., and Morrison, P. R. (1947) The conversion of human fibrinogen to fibrin under various conditions. *J. Am. Chem. Soc. 69*, 388–400.
31. Gabriel, D. A., Muga, K., and Boothroyd, E. M. (1992) The effect of fibrin structure on fibrinolysis. *J. Biol. Chem. 267*, 24259–24263.
32. Carr, M., and Alving, B. M. (1995) Effect of fibrin structure on plasmin-mediated dissolution of plasma clots. *Blood Coagulation Fibrinolysis 6*, 567–573.
33. Kim, P. Y., Stewart, R. J., Lipson, S. M., and Nesheim, M. E. (2007) The relative kinetics of clotting and lysis provide a biochemical rationale for the correlation between elevated fibrinogen and cardiovascular disease. *J. Thromb. Haemostasis 5*, 1250–1256.
34. Collet, J.-P., Lesty, C., Montalescot, G., and Weisel, J. W. (2003) Dynamic changes of fibrin architecture during fibrin formation and intrinsic fibrinolysis of fibrin-rich clots. *J. Biol. Chem. 278*, 21331–21335.
35. Yang, Z., Mochalkin, I., and Doolittle, R. F. (2000) A model of fibrin formation based on crystal structures of fibrinogen and fibrin complexed with synthetic peptides. *Proc. Natl. Acad. Sci. U.S.A. 97*, 14156–14161.
36. Kollman, J. M., Pandi, L., Sawaya, M. R., Riley, M., and Doolittle, R. F. (2009) Crystal structure of human fibrinogen. *Biochemistry 48*, 3877–3886.